Nanoscale

Cite this: *Nanoscale*, 2012, **4**, 3706

www.rsc.org/nanoscale

PAPER

Effects of potential environmental interferents on kinesin-powered molecular shuttles

Marlene Bachand[a] and George D. Bachand*[b]

Received 8th March 2012, Accepted 28th April 2012
DOI: 10.1039/c2nr30570d

Biomolecular motor-powered active transport represents an alternate means for analyte processing in nanoscale biosensors and bioanalytical devices. For example, a prototype "smart dust" biosensor has recently been reported in which the motor protein kinesin processes antibody-functionalized microtubules (MTs) to capture and separate optically tagged protein analytes. A potential limitation of this technology, however, involves the inhibition of transport function by interfering compounds that may be present in raw samples. Here we characterized the response of kinesin–MT transport to a range of potential interferents including solvents, acids, oxidizers, and environmental contaminants. The results of kinesin motility assays suggest that, among the tested interferents, only acetic acid and sodium hypochlorite adversely affected MT transport, primarily due to depolymerization of MT filaments. While negative effects were not observed for the remaining compounds tested, enhancement in motility was observed in the presence of acetone, antifreeze, and organic matter. Overall, the data suggest that kinesin–MT transport is resilient against a variety of common interferents, but primarily susceptible to failure due to significant changes in pH or the presence of an oxidizer.

1. Introduction

The miniaturization of sensors capable of handling micro- and nanoliter fluids has given rise to the concept of sensors capable of autonomous sample processing and detection. A key aspect to such "smart dust" devices is the ability to actively separate and transport analytes to a defined location in which they can be detected. Traditional approaches rely on fluid flow *via* pressure-driven or electrokinetic mechanisms that require power sources (*e.g.*, batteries), which significantly increase device size and weight.[1] To address this limitation, biomolecular motor-driven transport has been studied as an alternative means of separating and transporting analytes within sensor-based architectures. The uniqueness of this approach lies in materials transport in the absence of fluid flow. While the medium remains relatively static, the conversion of chemical energy into work (*i.e.*, nanofluidic transport) actively separates target from non-target analytes, enabling downstream detection and quantification.

A biomolecular motor-powered sensor for biological analytes can be envisioned as a basic linear process in which the kinesin motors and microtubule filaments (MTs) play three key roles: (i) analyte capture, (ii) analyte tagging, and (iii) analyte separation (Fig. 1). With respect to analyte capture, a number of approaches have been developed to selectively capture a range of bioanalytes using MT shuttles functionalized with either DNA[2–4] or antibodies.[5–9] The efficacy of capture is bounded by the time required for the analyte to diffuse to the functionalized MT, and the time required for the MT to move from the capture area to the tagging area. A key aspect of this transition is the separation of non-target analytes through kinesin active transport of MTs with captured analytes. Selective tagging represents the next critical phase in the process, and may be accomplished by forming a traditional immunological "sandwich."[6,9] Signal production in these sandwiches has been achieved using fluorescent spheres,[9] quantum dots,[6,10] engineered virus particles,[11,12] and fluorescent nucleic acid probes.[13] Following tagging, motor protein-transport separates the analytes from unbound tags, and moves the tagged analytes into a region in which detection can be achieved *via* optical spectroscopy or other means. The entire process, from capture to detection, can be achieved within minutes based on the velocity of the kinesin motors and a device size less than 1 millimeter.[1]

The application of kinesin-powered MT shuttles for detecting bioanalytes in environmental and clinical studies still faces a number of common challenges for new diagnostic platforms. For example, proteins such as kinesin and microtubules have limited lifetimes[14] and thermal stability.[15,16] Previous work also suggests that the lifetime of kinesin and microtubules may be significantly affected by the polymers used for device fabrication.[14] More critically, all of the aforementioned studies have used defined solutions of analytes in laboratory-prepared buffers, whereas field samples may contain interfering or inhibitory compounds. In this respect, the effects of potentially

[a]*Nanobiology Department, Sandia National Laboratories, PO Box 5800, Albuquerque, NM 87185, USA*
[b]*Center for Integrated Nanotechnologies, Sandia National Laboratories, PO Box 5800, MS 1303, Albuquerque, NM, 87185-1303, USA. E-mail: gdbacha@sandia.gov; Fax: +1 (505) 284-7778; Tel: +1 (505) 844-5164*

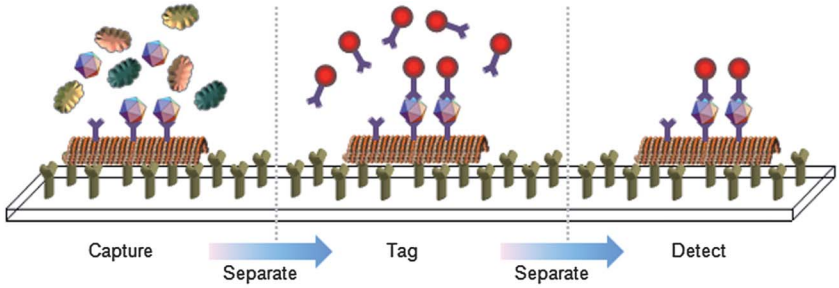

Fig. 1 Schematic representation of a nanoscale sensor capable of capturing, separating, and tagging biological analytes using kinesin biomolecular motor and antibody-functionalized microtubule shuttles to achieve nanofluidic transport.

confounding materials on antibody–antigen interactions have been widely studied,[17–20] and provide useful insight on how solvents, pH, and other factors may affect analyte capture/tagging in kinesin-based sensors. For example, the ionic strength of the solution strongly impacts the ionic interactions in antibody–antigen bonds, potentially giving false positive reactions.[19] Inhibition or deactivation of kinesin transport by interfering compounds, has not been reported, but represents a key technical issue as enzymatic function is commonly inhibited by contaminants such as humic acid.[21,22] Thus, the goal of this study was to determine the sensitivity of kinesin-driven molecular shuttles against a variety of potential interferents including common laboratory and environmental contaminants.

2. Experimental section

2.1 Kinesin and MT preparation

MTs were polymerized at 37 °C for 20–25 minutes using rhodamine tubulin (Cytoskeleton, Inc.) diluted in BRB80 buffer (80 mM PIPES pH 6.9, 1 mM $MgCl_2$, 1 mM EGTA) with 1 mM GTP and 10% glycerol. MTs were then stabilized by diluting 100-fold into BRB80T (BRB80 with 10 μM paclitaxel). MTs stabilized with 25 or 50 μM paclitaxel, or by 0.05% glutaraldehyde (GA) crosslinking[9,23] were also prepared and used to evaluate potential enhancement in MT stability in the presence of interferents. A histidine-tagged kinesin heavy chain motor was expressed from the pPK113 plasmid in *Escherichia coli* BL21 (DE3) pLysS, and purified on a Ni–NTA column as previously described.[24,25]

2.2 Interferent assays

Three general categories of interferents were investigated: acids/oxidizers, solvents, and environmental contaminants. Glacial acetic acid and sodium hypochlorite (*i.e.*, Chlorox® bleach) were selected as representative acids and oxidizers, respectively. Acetone, ethanol, methanol, and toluene were selected as solvents. Representative environmental contaminates included locally collected sandy soil, organic soil (Premier Pro-Mix®), gasoline (unleaded, 87 octane), and antifreeze (Prestone®). All interferents were diluted in motility buffer (BRB80 containing 0.2 mg mL^{-1} casein, 10 μM paclitaxel, 1 mM ATP, 20 mM dextrose, 0.02 mg mL^{-1} glucose oxidase, 0.008 mg mL^{-1} catalase, and 0.5% β-mercaptoethanol) to achieve 0.01%, 0.1%, or 1% concentrations.

Flow cells were constructed using a microscope slide, double-sided tape and a #1 glass coverslip. Casein (0.5 mg mL^{-1} in BRB80) was incubated in the flow cell for 5 minutes, followed by a solution of kinesin (~5 nM in BRB80 with 0.2 mg mL^{-1} casein and 1 mM ATP). MTs were flowed into the cell in motility solution and allowed to bind to kinesin for 10 minutes. The flow cell was then washed with fresh motility buffer to remove unbound MTs. Solutions containing the various concentration of interferents diluted in motility buffer were then added to the flow cells.

The effect of the interferents was characterized by epifluorescence using an Olympus IX71 microscope and 100× oil-immersion lens. Time-lapse and still frame images were collected using a Hamamatsu ORCA CCD camera. Data were collected within 30 min post-addition of motility solution containing the interferents; this timeframe is consistent with expected applications as previously discussed.[1] MT velocity was estimated by measuring the distance traveled between time-lapse images, and analyzed by one-way Analysis of Variance (ANOVA) to discern significant differences within the interferent treatments. If significant differences were present, comparisons among control and different concentrations of interferent treatments were analyzed with the Holm–Sidak method for multiple comparisons.

3. Results and discussion

Both acetic acid and sodium hypochlorite had substantial negative effects on the kinesin-transport of MT shuttles. Gliding MT velocity was significantly impacted by the presence of acetic acid in the motility solution (Fig. 2; $P < 0.001$). The 0.01 and 0.1% concentrations of acetic acid decreased the MT gliding velocity by ~13% and 36%, respectively. No MT motility was observed for the 1% concentration of acetic acid (Fig. 2). MT gliding velocity was also significantly impacted based on the concentration of sodium hypochlorite present in the motility buffer (Fig. 2; $P < 0.001$). No significant difference in the gliding velocity was observed between the negative control and 0.01% sodium hypochlorite solutions ($P = 0.796$). Higher concentrations of sodium hypochlorite (*i.e.*, 0.1 and 1%), however, resulted in the complete loss of MT transport. The lack of MT motility at the higher concentrations of sodium hypochlorite was primarily due to depolymerization of the MTs (Fig. 3). MT filaments are quite unstable with respect to factors such as temperature and the presence of divalent metal ions.[26–30] The observed MT

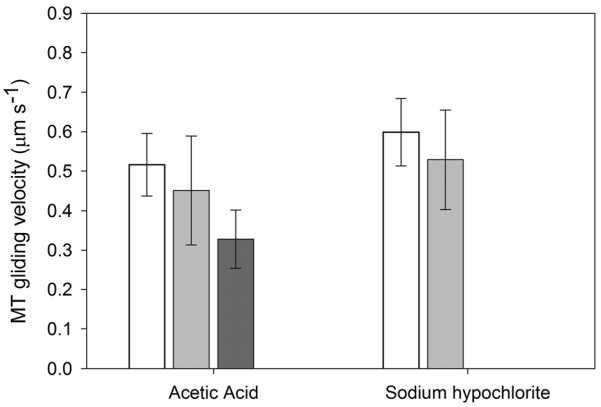

Fig. 2 Velocity of gliding MTs in motility buffer containing 0 (white), 0.01 (light grey), 0.1 (medium grey), and 1% (dark grey) acetic acid or sodium hypochlorite. Mean ± standard deviation.

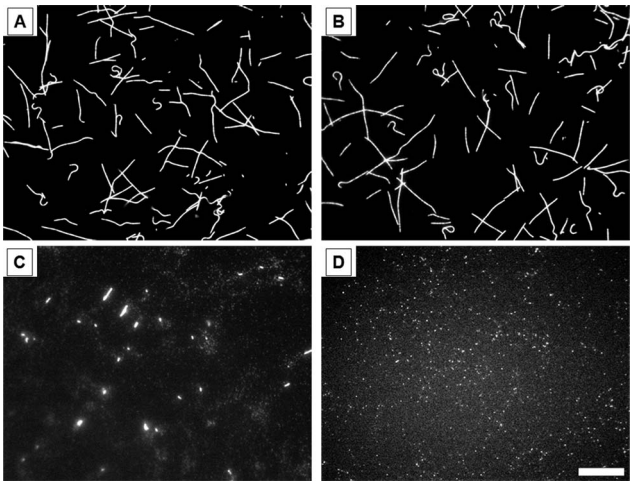

Fig. 3 Images of MT filaments exposed to 0 (A), 0.01 (B), 0.1 (C), and 1% (D) concentrations of sodium hypochlorite. Scale bar = 25 μm.

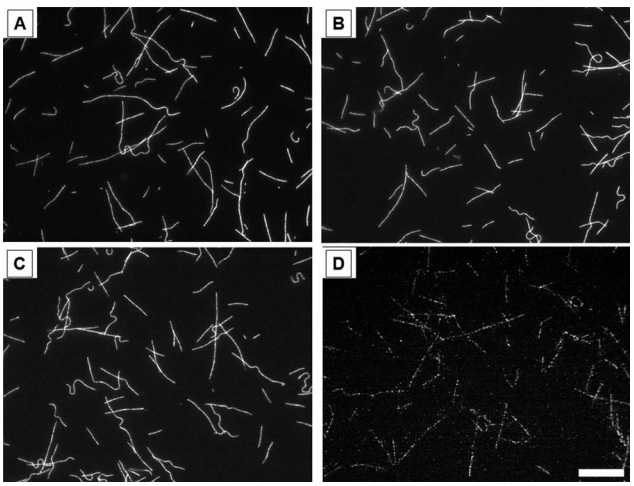

Fig. 4 Images of MT filaments exposed to 0 (A), 0.01 (B), 0.1 (C), and 1% (D) concentrations of acetic acid. Scale bar = 25 μm.

depolymerization in the presence of 0.1 and 1% sodium hypochlorite was likely due to the susceptibility of amino acids to oxidation.[31,32] Thus, while the kinesin motors may have remained active under these conditions, the depolymerization of MTs equates to a loss in transport function with respect to a sensor-based system. In contrast, MTs could be observed attached to the kinesin surface across all concentrations of acetic acid (Fig. 4), despite a complete lack of motility at the highest (*i.e.*, 1%) concentration. The fluorescence of MTs in the 1% acetic acid solution was quite punctate (Fig. 4D), suggesting that the MTs are depolymerizing. While the fluorophore may be sensitive to acidic pHs, a uniform decrease in photo-luminescence across the MT, as opposed to the observed punctate fluorescence, would have been expected in response to pH-related effects. The pH values of motility solutions containing 0.01%, 0.1%, and 1% acetic acid were 6.9, 6.6, and 4.5, respectively; the pH of all solutions containing sodium hypochlorite remained at pH 6.9. Based on these data, we conclude that the loss of MT transport is due to pH-based inactivation of the kinesin motors. Similar findings have been observed for kinesin–MT transport the presence of strongly basic developers used in microfabrication processes.[28] Moreover, the functional range of kinesin motor activity have been reported within a pH range of 6.0–7.8.[33]

Increased concentrations of paclitaxel, as well as GA crosslinking, were evaluated as potential mitigators of acetic acid and sodium hypochlorite effects. MTs stabilized with 10, 25, and 50 μM paclitaxel or crosslinked with 0.05% GA were characterized before and after exposure to motility solutions containing either 1% acetic acid or 1% bleach. MT morphology and motility were monitored at regular intervals for 45 minutes post-exposure to evaluate time-dependent effects. Increased MT stability in motility solution containing 1% acetic acid (pH 4.5) was observed for MTs stabilized with 25 and 50 μM paclitaxel, as well as MTs crosslinked with GA (Fig. 5). These observations are consistent with paclitaxel-enhanced stability of MTs at alkaline pHs that has been previously reported.[34] While MT morphology was maintained up to 45 min after exposure to acetic acid, kinesin-based transport of MTs was never observed, further suggesting inactivation of motor function at acidic pH values. MTs stabilized with 50 μM paclitaxel showed increased stability against sodium hypochlorite (Fig. 5); whereas, the 10 and 25 μM paclitaxel-stabilized, and GA crosslinked MTs experienced complete MT depolymerization within 20 min post-introduction (Fig. 5). Despite the maintenance of morphology, MTs stabilized with 50 μM paclitaxel disassociated from the surface (kinesin) over time, suggesting that sodium hypochlorite affected interactions at the kinesin–MT binding site. Moreover, motility of these MTs was never observed, which may be attributed to inactivation of the kinesin motor function due to amino acid oxidation. In summary, increased MT stability against acetic acid and sodium hypochlorite could be achieved with increased concentrations of paclitaxel. Kinesin motor function, however, was not maintained under these conditions, thus significantly impacting the overall transport system.

MT transport was minimally affected by the presence of the various solvents in the motility solution (Fig. 6). No significant differences in gliding velocity were observed for ethanol, methanol, and toluene ($P > 0.05$), regardless of concentration. The MTs in these assays did not show visual signs of degradation

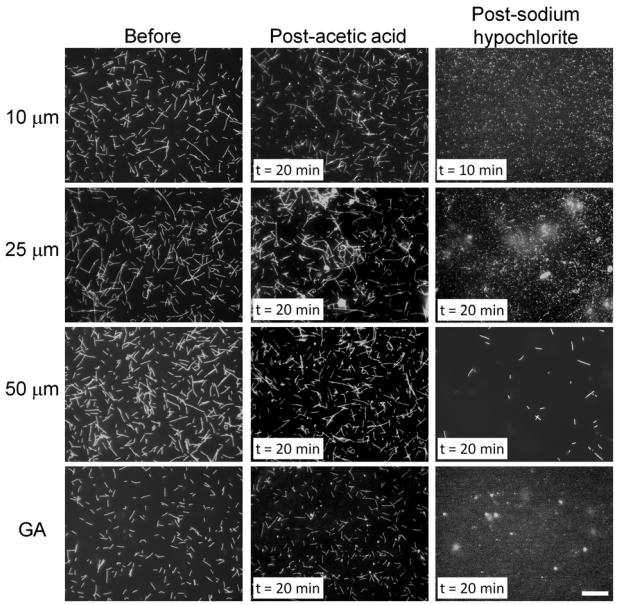

Fig. 5 Images of MT filaments before and after exposure to 1% solutions of acetic acid and sodium hypochlorite. MTs were stabilized with 10, 25, or 50 μM concentrations of paclitaxel, or crosslinked with 0.05% glutaraldehyde (GA). t = time post-introduction. Scale bar = 25 μm.

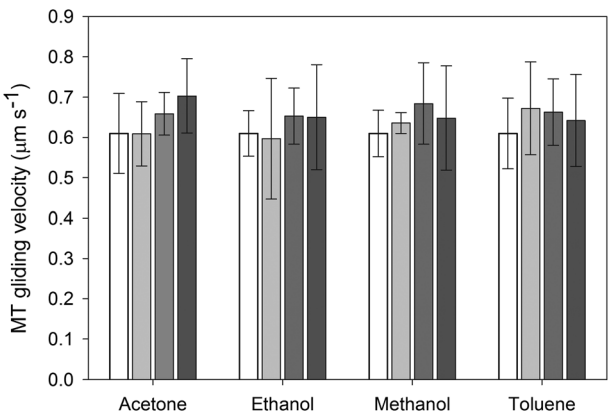

Fig. 6 Velocity of gliding MTs in motility buffer containing 0 (white), 0.01 (light grey), 0.1 (medium grey), and 1% (dark grey) acetone, ethanol, methanol, or toluene. Mean ± standard deviation.

and/or depolymerization, as compared with the negative control. A significant difference in gliding velocity was observed, however, for acetone ($P < 0.003$). In contrast to the negative effect of sodium hypochlorite and acetic acid, kinesin–MT transport displayed significant increases in velocity based on the concentration of acetone (Fig. 6). More specifically, the gliding velocity was significantly higher for the 1% concentration of acetone when compared against the negative control and 0.01% acetone samples ($P < 0.05$). No differences were observed among the negative control, 0.01% and 0.1% acetone samples ($P > 0.200$). The MTs did not visually differ in appearance across all concentrations of acetone when compared with the control sample. Such an effect on kinesin transport was not observed in a related study in which MT gliding was characterized in the presence of 20% acetone.[28] The critical conclusion from these findings, however, indicates that kinesin transport is not adversely impacted by the presence of the tested solvents. Putative enhancement of motility by acetone remains unclear and requires further investigation.

Two of the four environmental contaminants had significant effects on kinesin–MT transport (Fig. 7). Both antifreeze and organic matter significantly affected ($P < 0.001$) the gliding velocity of MT shuttles, whereas sandy soil and gasoline had no effect ($P > 0.1$). Similar to the observations for acetone, the gliding MT velocity displayed increased rates for both antifreeze and organic matter. For the former, MT velocity increased by ~10% for the 0.01% concentration of antifreeze, but was not significantly different from the control ($P = 0.08$). The velocity significantly increased, as compared against the control, by approximately 30 and 37% for the 0.1 and 1% concentrations of antifreeze, respectively ($P < 0.001$). The primary components of antifreeze include ethylene glycol and propylene glycol, which serve as osmolytes. The role of protein solvation in enzyme catalysis has been studied through the use of osmolytes such as ethylene glycol and polyethylene glycol (PEG).[35–38] For example, increased activity was reported for hexokinase and glucose-6-phosphate dehydrogenase in the presence of low molecular weight PEG (*i.e.*, PEG).[36,39] The effect was reversed in hexokinase by higher molecular weight PEG (*e.g.*, PEG1500 and PEG4000) molecules, which reduced activity by up to 15% based on induced unfolding and aggregation.[36] Enhanced catalysis associated with ethylene glycol has been reported for myosin motors,[35] suggesting that the ethylene glycol in antifreeze may be responsible for the enhanced MT gliding velocities observed in our experiments.

Similar increases in MT gliding velocities were observed as a function of the different concentrations of organic matter added to the motility buffer (Fig. 7). The gliding motility velocities of the three treatments significantly differed from velocity of the control ($P < 0.001$), and displayed increases of approximately 25%, 34%, and 35% for the 0.01, 0.1, and 1% concentrations of organic matter, respectively. Humic acids found in organic matter are often inhibitory to enzyme function,[21,40] but may also be stimulatory as in the case of certain degradative enzymes.[40,41] While our experiments suggest that

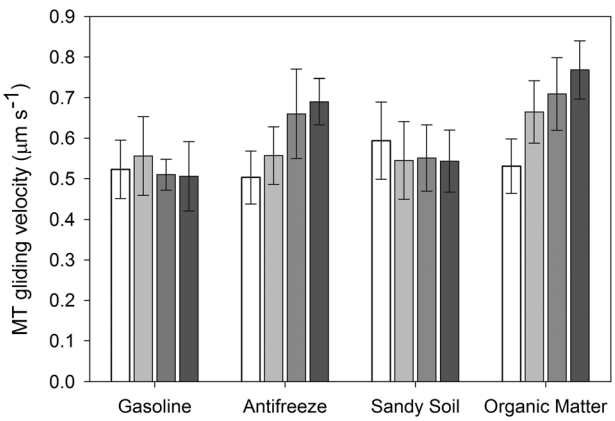

Fig. 7 Velocity of gliding MTs in motility buffer containing 0 (white), 0.01 (light grey), 0.1 (medium grey), and 1% (dark grey) gasoline, antifreeze, sandy soil, or organic matter. Mean ± standard deviation.

kinesin activity is stimulated by a component in the organic matter, the nature of this enhancement cannot be directly linked with one or more components of the organic matter based on the intrinsically complex mixture of organic and inorganic constituents. Establishing cause–effect relationships would require compositional analyses of various organic soils and subsequent correlation analyses between compositional differences and/or similarities with enhancement in gliding motility. The key observation from our data, however, resides in a lack of inhibition that is commonly associated with environmental samples containing organic matter.

4. Conclusions

We have characterized the effect of potential interferents on the kinesin–MT transport system that has been used in smart dust biosensor applications. Kinesin transport was unaffected by most of the interferents tested with the exception of acetic acid and sodium hypochlorite, which induced MT depolymerization, reduced MT gliding velocity, and inactivated motor function at high concentrations. Overall these results suggest that the application of kinesin transport in hybrid sensor-device should be quite resilient with respect to processing more complex samples than have previously been tested. Evaluation of additional interferents will be needed in the future to ensure unaffected function in specific sample types and composition. In addition, time-dependent effects of potential interferent will need to be addressed for applications that may require >30 min of transport duration. Lastly, the continued development of kinesin-based sensor architectures must anticipate and assess potential interference by contaminating materials such as soil particles that may ultimately affect performance.

Acknowledgements

We thank Darryl Sasaki and Erik Spoerke for helpful discussion and comments on this manuscript, and Dr Joe Howard for generously providing the Drosophila kinesin expression clone. This research was supported by the Defense Advanced Research Projects Agency (M.B.) and U.S. Department of Energy, Office of Basic Energy Sciences, Division of Materials Sciences and Engineering, Project KC0203010 (G.D.B.). This work was performed, in part, at the Center for Integrated Nanotechnologies, a U.S. Department of Energy, Office of Basic Energy Sciences user facility. Sandia National Laboratories is a multi-program laboratory operated by Sandia Corporation, a wholly owned subsidiary of Lockheed Martin company, for the U.S. Department of Energy's National Nuclear Security Administration under contract DE-AC04-94AL85000.

References

1 G. D. Bachand, H. Hess, B. Ratna, P. Satir and V. Vogel, *Lab Chip*, 2009, **9**, 1661–1666.
2 S. Hiyama, R. Gojo, T. Shima, S. Takeuchi and K. Sutoh, *Nano Lett.*, 2009, **9**, 2407–2413.
3 S. Taira, Y. Z. Du, Y. Hiratsuka, T. Q. P. Uyeda, N. Yumoto and M. Kodaka, *Biotechnol. Bioeng.*, 2008, **99**, 734–739.
4 S. Hiyama, T. Inoue, T. Shima, Y. Moritani, T. Suda and K. Sutoh, *Small*, 2008, **4**, 410–415.
5 L. Rios and G. D. Bachand, *Lab Chip*, 2009, **9**, 1005–1010.
6 T. Fischer, A. Agarwal and H. Hess, *Nat. Nanotechnol.*, 2009, **4**, 162–166.
7 A. Carroll-Portillo, M. Bachand and G. D. Bachand, *Biotechnol. Bioeng.*, 2009, **104**, 1182–1188.
8 S. Ramachandran, K.-H. Ernst, G. Bachand, V. Vogel and H. Hess, *Small*, 2006, **2**, 330–334.
9 G. D. Bachand, S. B. Rivera, A. Carroll-Portillo, H. Hess and M. Bachand, *Small*, 2006, **2**, 381–385.
10 L. Rios and G. D. Bachand, *Lab Chip*, 2009, **9**, 1005–1010.
11 B. D. Martin, C. M. Soto, A. S. Blum, K. E. Sapsford, J. L. Whitley, J. E. Johnson, A. Chatterji and B. R. Ratna, *J. Nanosci. Nanotechnol.*, 2006, **6**, 2451–2460.
12 C. M. Soto, B. D. Martin, K. E. Sapsford, A. S. Blum and B. R. Ratna, *Anal. Chem.*, 2008, **80**, 5433–5440.
13 M. Hirabayashi, S. Taira, S. Kobayashi, K. Konishi, K. Katoh, Y. Hiratsuka, M. Kodaka, T. Q. P. Uyeda, N. Yumoto and T. Kubo, *Biotechnol. Bioeng.*, 2006, **94**, 473–480.
14 C. Brunner, K. H. Ernst, H. Hess and V. Vogel, *Nanotechnology*, 2004, **15**, S540–S548.
15 K. J. Böhm, R. Stracke, M. Baum, M. Zieren and E. Unger, *FEBS Lett.*, 2000, **466**, 59–62.
16 S. B. Rivera, S. J. Koch, J. M. Bauer, J. M. Edwards and G. D. Bachand, *Fungal Genet. Biol.*, 2007, **44**, 1170–1179.
17 D. R. Absolom and C. J. Vanoss, *CRC Crit. Rev. Immunol.*, 1986, **6**, 1–46.
18 M. Rehan and H. Younus, *Int. J. Biol. Macromol.*, 2006, **38**, 289–295.
19 R. Reverberi and L. Reverberi, *Blood Transfus.*, 2007, **5**, 227–240.
20 J. H. Skerritt, A. S. Hill, R. B. S. Rao, H. L. Beasley, B. E. A. Rani, C. G. U. Kumari, Y. N. Vijayashankar, N. B. R. K. Venugopal and N. G. K. Karanth, *Food Agric. Immunol.*, 2003, **15**, 17–34.
21 M. Harry, B. Gambier, Y. Bourezgui and E. Garnier-Sillam, *Analusis*, 1999, **27**, 439–442.
22 J. B. Jahnel, B. Mahlich and F. H. Frimmel, *Acta Hydrochim. Hydrobiol.*, 1994, **22**, 109–116.
23 A. Boal, H. Tellez, S. Rivera, N. Miller, G. Bachand and B. Bunker, *Small*, 2006, **2**, 793–803.
24 G. D. Bachand, S. B. Rivera, A. K. Boal, J. Gaudioso, J. Liu and B. C. Bunker, *Nano Lett.*, 2004, **4**, 817–821.
25 D. L. Coy, M. Wagenbach and J. Howard, *J. Biol. Chem.*, 1999, **274**, 3667–3671.
26 B. Vulevic and J. J. Correia, *Biophys. J.*, 1997, **72**, 1357–1375.
27 P. B. Schiff, J. Fant and S. B. Horwitz, *Nature*, 1979, **277**, 665–667.
28 V. Verma, W. O. Hancock and J. M. Catchmark, *IEEE Trans. Adv. Packag.*, 2005, **28**, 584–593.
29 G. Galella and D. B. Smith, *Can. J. Biochem. Cell Biol.*, 1979, **57**, 1368–1375.
30 C. S. Regula, J. R. Pfeiffer and R. D. Berlin, *J. Cell Biol.*, 1981, **89**, 45–53.
31 L. M. Landino, R. Hasan, A. McGaw, S. Cooley, A. W. Smith, K. Masselam and G. Kim, *Arch. Biochem. Biophys.*, 2002, **398**, 213–220.
32 G. Cappelletti, B. Pedrotti, M. G. Maggioni and R. Maci, *Cell Biol. Int.*, 2001, **25**, 981–984.
33 K. J. Böhm, R. Stracke and E. Unger, *Cell Biol. Int.*, 2000, **24**, 335–341.
34 I. Ringel and S. B. Horwitz, *J. Pharmacol. Exp. Ther.*, 1991, **259**, 855–860.
35 G. Kaldor, *Arch. Biochem. Biophys.*, 1968, **127**, 22–30.
36 S. M. Pancera, R. Itri and D. F. S. Petri, *Prog. Colloid Polym. Sci.*, 2004, **128**, 178–183.
37 R. P. Rand, N. L. Fuller, P. Butko, G. Francis and P. Nicholls, *Biochemistry*, 1993, **32**, 5925–5929.
38 C. Reid and R. P. Rand, *Biophys. J.*, 1997, **72**, 1022–1030.
39 L. Laan, J. Husson, E. L. Munteanu, J. W. J. Kerssemakers and M. Dogterom, *Proc. Natl. Acad. Sci. U. S. A.*, 2008, **105**, 8920–8925.
40 A. H. Vuorinen and M. H. Saharinen, *Soil Biol. Biochem.*, 1996, **28**, 1477–1481.
41 B. Kluczek-Turpeinen, P. Maijala, M. Tuomela, M. Hofrichter and A. Hatakka, *World J. Microbiol. Biotechnol.*, 2005, **21**, 1603–1609.

